Specific Features of the Carbon Nanotubes Nucleation and Growth in the Porous Alumina Membrane

Alla Vorobjova[1], Alena Prudnikava[2], Yuri Shaman[3], Boris Shulitski[4], Vladimir Labunov[5], Sergey Gavrilo[6], Alexey Belov[7], Alexander Basaev[8]

[1,2,4,5]Belarusian State University of Informatics and Radioelectronics, P. Brovka St. 6, Minsk, 220013 Belarus
[3]Scientific Manufacturing Complex Technological Center MIET, Moscow, Zelenograd, 4806th, 124498 Russia
[6,7,8]National Research University of Electronic Technology, Proezd, 5, Moscow, Zelenograd, 4806th, 124498 Russia
[1]vorobjova@bsuir.by; [2]prudnikova@bsuir.by

***Abstract*-Aligned, highly uniform multiwall carbon nanotubes (MWCNT) in a porous anodic aluminum oxide (AAO) membrane were successfully grown by chemical vapor deposition (CVD). The effectiveness of MWCNT formation was studied with various synthesis parameters. It was found that high catalyst (ferrocene) concentrations led to formation of a thick layer of MWCNT arrays on top surface of AAO membranes, which led to decrease of the pores filling with nanotubes. It was shown that the growth mechanism of the nanotubes in the AAO pores by this method was not connected with the traditionally used transition metal catalysts, no matter whether they were in a deposited (localized catalyst) or volatile (injected catalyst) state. The pre-annealing process in air atmosphere inhibited the nanotubes formation in the AAO pores. We speculate that the formation of MWCNT s in the AAO pores is governed by the pore structure reconstruction (water desorption, phase transformation) during the high-temperature (870 °C) CVD process, though this phenomenon needs further investigation.**

Keywords- Chemical Vapour Deposition; Carbon Nanotubes; Porous Aluminum Oxide; Ferrocene; Xylene

I. INTRODUCTION

Arrays of carbon nanotubes (CNTs) embedded in porous anodic aluminum oxide (AAO) are of essential interest as active elements in field emission cathodes [1-4] and chemical and biological sensors [5-7]. "Nanovials" manufactured from the resulting composite can be easily filled, for example, with ferromagnetic materials. They are well dispersed in water and ethyl alcohol and can be used in medicine for drug delivery in vivo [8]. Nanotubes synthesized in the AAO pores possess increased adsorption properties when compared with the known carbon material, such as activated carbon, single- and multi-wall CNTs and can be used for the creation of hydrogen storage containers [9]. According to different publications, aligned CNTs can be synthesized in a porous anodic AAO with [10, 11] and without catalysts [12, 13]. In general, a localized catalyst (Ni, Fe, Co) electrochemically deposited into AAO pores is used for the CNT synthesis over a thin-film AAO/substrate (dielectric or silicon). If the AAO films with through pores (membranes) are used, the synthesis is performed with volatile catalysts, since the electrochemical metal deposition into the pores with high aspect ratio represents a complex technological task. However, the results presented in different publications are contradictory and do not yield an unambiguous idea of the catalyst influence and CNT growth mechanism in the porous AAO.

In this study, we considered the synthesis of aligned carbon nanotubes in the AAO pores by the injection chemical vapour deposition (CVD) method with both types of catalysts (localized and injected). The optimal conditions for the pores filling with nanotubes were determined. The effect of CVD synthesis conditions, as well the role of localized catalyst on the CNT nucleation and growth were studied.

II. EXPERIMENTAL

A. Synthesis of the AAO Template

The specially prepared porous AAO membranes consist of a self-ordered array of closely packed hexagonal cells containing cylindrical pores with high degree of homogeneity. Samples of 99.95% aluminum foil with a thickness of 100 ± 5 μm and a size of 3 × 4 cm were used as the initial material for the manufacture of porous AAO templates. Before anodization, the samples were chemically polished in a mixture of orthophosphoric and nitric acids in a proportion of 8:1 at a solution temperature of 80 ± 2°C for 1 min. The foil thickness after polishing was 90 ± 5 μm. The porous anodization of foil samples was performed with a two-stage method [14] in a 4% water solution of oxalic acid. At the first stage, porous AAO with a thickness of about 50 μm was formed in the high-voltage regime [15]. Then the formed AAO was chemically removed in the selective etchant (35 ml/l of 85% H3PO4 + 20 g/l of CrO3) at a temperature of 80 ± 2 ℃. The second stage of anodization was performed until the aluminum foil was completely oxidized. To provide the electric regime in anodization, the stabilized analog power supply TEC 5818 was used. The forming voltage was established by scanning with a constant rate of 0.5 V/s.

DOI: 10.5963/AMSA0302001

The electrolyte temperature (10 ℃) was kept constant with a precision of ±2.0 ℃. The membranes obtained in this regime contained pores with a diameter of 50–60 nm. The membrane's thickness was 42 μm with a porous structure having aspect ratio of about 840.

After anodization, the AAO pore walls were chemically polished in a 4% water solution of H3PO4 at room temperature for 40 min; this resulted in a pore expansion and etching of the barrier oxide layer on the pore bottom. This procedure reduces the degree of roughness of the pore inner surface too, which is important for the CNT deposition. After polishing, the pore diameter increased to 80–90 nm. Then, by means of magnetron sputtering one side of the porous AAO membrane was covered with a nickel film with a thickness of 30 nm (localized catalyst). These AAO membranes were subsequently subjected to the CVD process with injected catalyst.

B. Synthesis of CNTs

CNTs were synthesized using injection CVD method by means of a high-temperature pyrolysis of liquid hydrocarbon (xylene [C8H10]) mixed with the volatile catalyst source (ferrocene [Fe(C5H5)2]). This process was performed at atmospheric pressure in an Ar/NH3 flow. Ammonia addition was supposed to facilitate the catalytic activity of Ni particles formed from the sputtered film at the high temperature synthesis conditions. The ferrocene concentration in xylene was 0.1–10(wt.)%, the injection rate of the reaction mixture into the reactor zone was 1 ml/min, the temperature was 870 ℃, the argon flow rate was 100 cm3/min, and the flow rate of NH3 was 10 cm3/min. The synthesis duration was 1–10 min.

The experimental results for four CNT synthesis regimes are: in regime I, 1% feeding solution was injected for 1 min; in regime II, these parameters were 10% and 1 min; and in regime III, 0.1% and 1 min, respectively. In regime IV, 1% feeding solution was injected for 1 min but without NH3 supply. Thus, regime I differs from regime II only by the used feeding solution concentration, and regime I differs from regime IV by the NH3 addition to the carrier gas flow.

C. Characterization Techniques

The morphology and structure of the samples were investigated by scanning electron microscopy, SEM (Phillips XL30 S FEG and Hitachi S-4800), transmission electron microscopy, TEM (Phillips CM-30), Raman spectroscopy (LabRam Aramis Raman Spectrometer, Horiba Scientific, laser wavelength λ=532 nm), and Auger electron spectroscopy (spectrometer PHI 660).

III. RESULTS AND DISCUSSION

A. The Effect of CVD Regime

It was observed that the AAO membranes after the CNT synthesis process using the feeding solution concentrations of 1-10% appeared to be covered with a thick layer of entangled CNT arrays. Fig. 1 shows SEM images of the samples obtained in regime I: as-synthesized (Fig. 1(A)) and after mechanical cleaning of the AAO surface from the CNT crust on top (Fig. 1(B)).

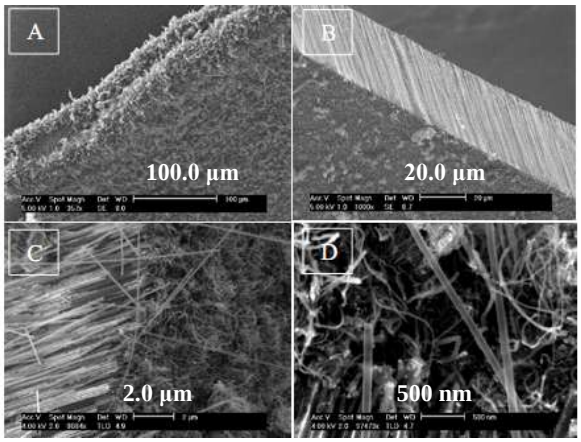

Fig. 1 SEM images of the AAO membranes after CNT synthesis in regime I (A) as-synthesized; (B) after mechanical cleaning of the top CNT crust; (C, D) magnified views of the AAO cross section showing the nanotubes grown on top and in the pores

CNTs formed on the AAO surface begin to grow actively only if the ferrocene concentration increases to 1.0% and higher (regime I). These CNTs produced on the surface of the sample have significantly smaller diameters (from 10 to 20 nm) than that grown inside AAO since it is not controlled by the pore size of the AAO membrane (Fig. 1(C, D)). The difference observed in the carbon material formed on the sample surface and in the AAO pores is governed by the peculiarities of their formation mechanism.

It is seen in Fig. 2(A, B) that the aligned nanotubes repeating the pore shape were formed in the AAO membrane. It is noteworthy that the diameter of the pores appeared to be slightly increased to 70-100 nm (regime III) or 100-130 nm (regime I), depending on the initial pore diameter after the CVD process. The nanotubes were open-ended, the internal diameter was about

DOI: 10.5963/AMSA0302001

50–70 nm, and they did not contain visible structural defects.

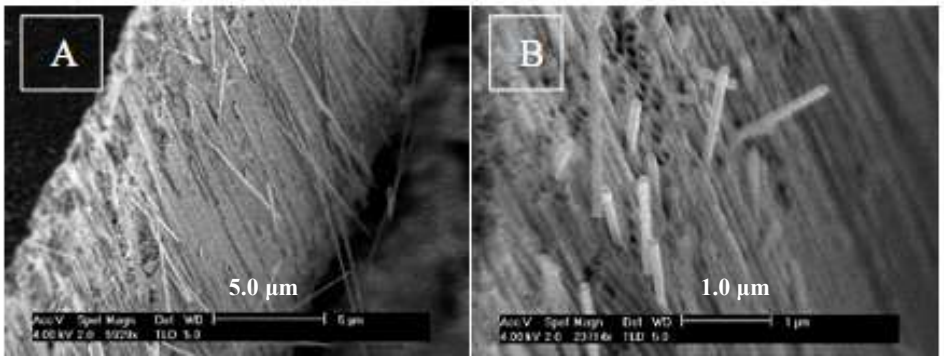

Fig. 2 A, B SEM images (A, B) of the AAO cross section showing the nanotubes grown in the pores in regime I

For comparison, SEM images of the sample obtained in regime II are presented in Fig. 3. This regime differs from regime I only by a higher feeding solution concentration. It is noticeable that there were fewer nanotubes feeling the pores (Fig. 3(A)) which may be caused by a very thick CNT crust layer grown on top of the membrane (Fig. 3(B)) which hindered the diffusion of the feedstock into the pores thus preventing the nanotube formation.

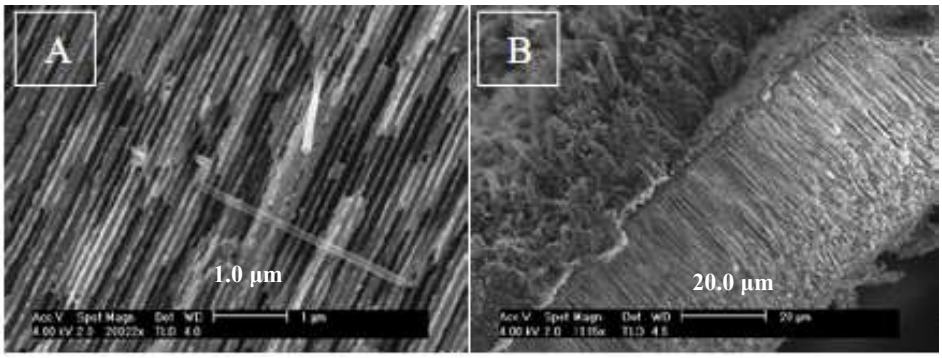

Fig. 3 SEM images of AAO membranes after CNT synthesis in regime II (A) A few nanotubes protruding from the AAO pores; (B) general view of the sample with a 30 µm CNT crust layer on top

In order to eliminate the formation of the CNT crust layer, the synthesis in regime III was conducted with the reduced concentration of ferrocene in the feeding solution but with longer deposition time (Fig. 4(A-C)). As a result, the nanotubes were formed in almost all the pores of AAO.

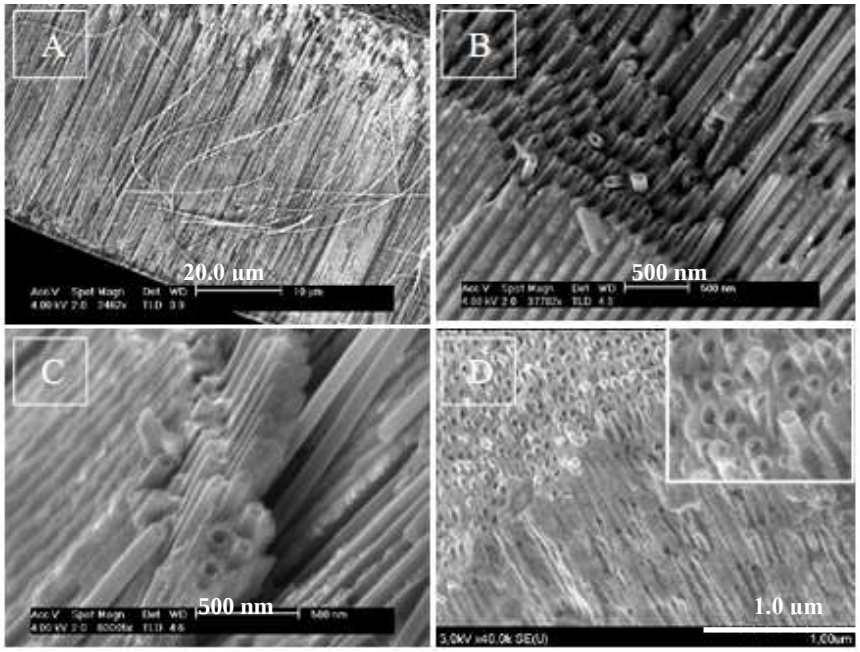

Fig. 4 SEM images of the AAO membranes after CNT synthesis in regime III (A-C) and regime IV (D and the inset)

DOI: 10.5963/AMSA0302001

Furthermore, the effect of ammonia was investigated. For this purpose, we repeated the regime I, but excluded NH_3 from the gas flow (regime IV). It was revealed that the nanotubes having much thinner walls were formed in the AAO pores (Fig. 4(D) and the inset).

Based on the results of SEM investigation presented it can be concluded that in the samples obtained in different synthesis regimes, the aligned carbon nanotubes repeating the pore shape are formed within a porous AAO membrane. If the ferrocene concentration increases by up to 1.0% and higher, an entangled CNT layer having much smaller nanotube diameters is formed on the AAO surface. The catalyst precursor concentration used for the synthesis process increases the thickness of CNT layer on top of AAO increases, preventing the diffusion of carbon feedstock into the pores, and thus restricting the nanotubes growth inside the AAO pores. The addition of NH3 into the gas flow promotes the thickening of the nanotube walls. The conditions of regime III are considered as optimal for the nanotube formation in the AAO pores. However, the role of Ni as catalyst was not evidenced by SEM studies.

B. The Structural Properties of Nanotubes

For TEM analysis, the samples were first mechanically ground, sonicated in isopropyl alcohol, and then put onto a copper grid. The difference in the geometric size and shape of the nanotubes formed inside the membrane and on its surface is clearly illustrated in Fig. 5. Fig. 5(A) shows TEM images of the nanotubes formed in the pores of AAO in regime IV. They have relatively large diameters of about 130 nm and look brittle. During TEM analysis, lots of damaged and unzipped nanotubes rather like graphene flakes (pointed with an arrow in Fig. 5(A)) were found. In Fig. 5(B) along with the nanotubes grown in the AAO pores (1) the carbon nanotubes (2) grown on the surface of AAO membrane are indicated. This kind of nanotubes has diameters of about 20-60 nm and even has catalyst nanoparticles inclusions in their channels (indicated with arrows, Fig. 5(B)).

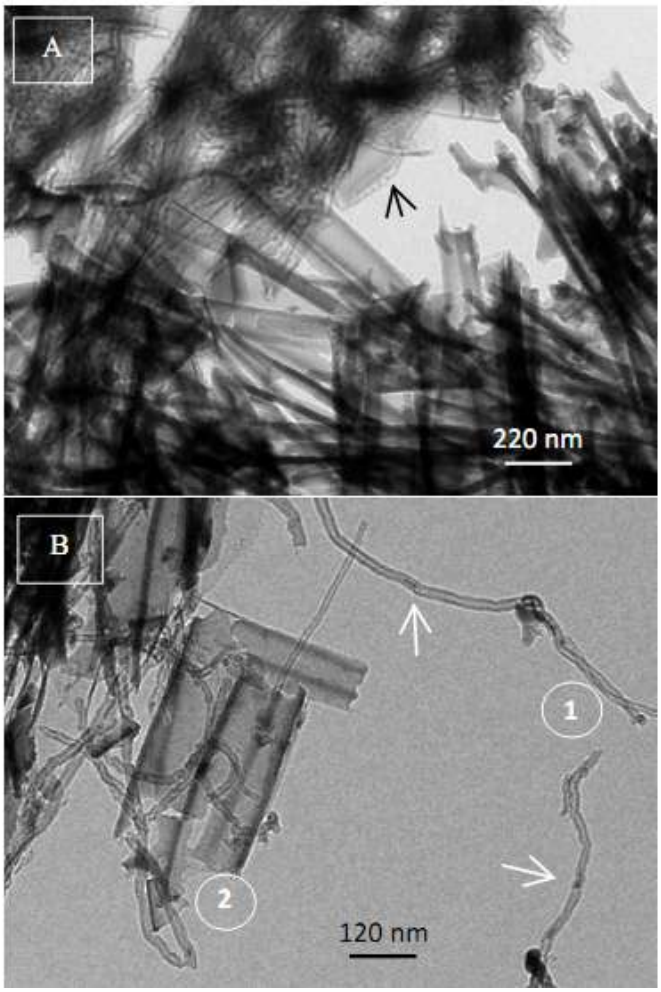

Fig. 5 TEM images of the nanotubes of two types: (A) nanotubes grown inside the AAO pores; (B) classical CNTs drown on the AAO surface (1) and the nanotubes grown inside the AAOpores (2). With arrows the catalyst nanoparticles are indicated

This is the evidence that these CNTs are classical for they were grown via extrusion of graphite fraction from carbide phase (most likely, iron carbide from ferrocene decomposition) of catalytic nanoparticles during CVD [16]. The growth mechanism of the tubes formed in the pores will be discussed later.

For the investigation of the structure of the nanotubes formed in the AAO pores, the samples were studied by Raman

DOI: 10.5963/AMSA0302001

spectroscopy. Fig. 6(A) shows the typical Raman spectra of the pristine AAO and the AAO sample after the CNT synthesis (regime I) followed by surface cleaning. After synthesis, Raman spectrum exhibited two distinct peaks at 1590 and 1355 cm^{-1} which are the feature of graphitic materials. The band at 1550-1605 cm^{-1} (G band) is attributed to E_{2g} symmetry in-plane optical mode associated with the stretching of all C=C pairs, while the band near 1350 cm^{-1} (D band) is physically related to the in-plane A_{1g} symmetry breathing mode of the C hexagon which intensifies and broadens when the amount of structural defects increases. The ratio ID/IG obtained after the background subtraction and fitting with two Gaussians is 0.83, which is lower than that obtained for the nanotubes grown in AAO using C_2H_2 decomposition [17] yet still quite high. This ratio may indicate a semicrystalline carbon structure with some plane defects and lattice edges. Unfortunately, the way of stacking order of graphitic planes cannot be estimated from this data as the G' band is out of the measured range, but most probably it is similar to turbostratic graphite [18].

The elemental composition on a surface and in the volume of the samples synthesized in a regime III was investigated by the Auger spectroscopy with profiling along the membrane depth after the mechanical cleaning of its surface. The uniform distribution of basic elements – Al, O, and C along the sample depth was established, with relative atomic concentrations of 29, 54 and 18%, respectively (Fig. 6(B)). Neither nickel nor iron, from the decomposed ferrocene was detected.

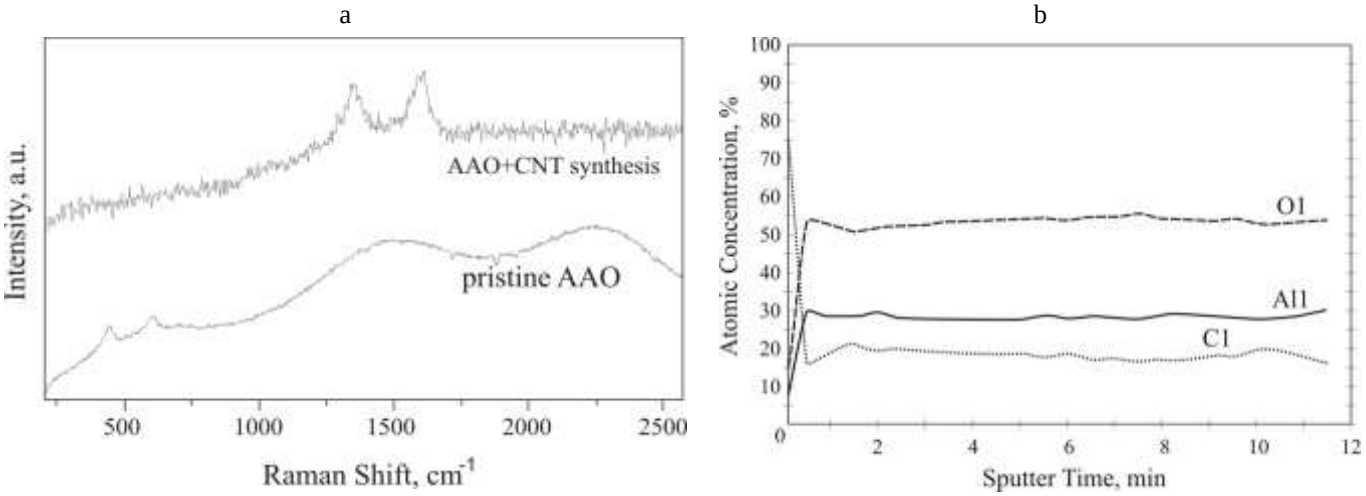

Fig. 6 Raman (a) and Auger electron (b) spectra recorded from the sample obtained in regime III (after the surface cleaning)

C. Specific Features of the Nanotubes Growth

The results show that there are important specific features of the high temperature reconstruction of the AAO pores during CVD process. In our previous work the changes in the AAO chemical composition and structure after the high-temperature CVD process were studied by X-ray photoelectron spectroscopy (XPS) [19]. In-depth analysis of the core C *1s*- and Al *2p*-levels revealed (along with C-C, C-O and Al^{3+}) the presence of Al-C and Al^0 in the analysed sample. This indicated that AAO itself was involved in the physical and chemical process of CNT formation in its pores. The fact that the pore diameter was slightly increased after the synthesis supported this argument.

Indeed, the AAO membrane obtained with the use of oxalic acid may contain 6-10% of adsorbed water, and bound water ($Al_2O_3 \cdot nH_2O$, n=1-3). The former was desorbed at 110-130 ℃, and the latter at 350-550 ℃. This explains the enlargement of the pore diameter after the synthesis process. Moreover, during the synthesis process at temperatures up to 900 ℃ in the AAO pore Al was partially reduced and partially transformed into a crystalline γ-Al_2O_3 phase [20], which was accompanied by the shrinkage of its volume. Since aluminum carbides can be formed directly from aluminum oxide by reacting with carbon at significantly higher temperatures (~1800 ℃), we suggest that only the released after the water desorption Al can react with carbon species from the gas phase thus forming carbide (most probably, Al_4C_3). As long as Al_4C_3 is stable at up to 1400 ℃, it exists along with the polycrystalline γ- Al_2O_3 and probably $C_2O_4^{2-}$ anions as a residual from the electrolyte solution, and can support or even take part in the formation of the nanotubes in the pores during CVD.

It is noteworthy that at similar synthesis conditions described in [19], neither Ni nor Fe was detected in the pores by XPS. Therefore, it raises the question that whether nickel particles formed on one side of AAO and iron particles from the ferrocene decomposition participate in the formation of nanotubes in the AAO pores. It is obvious though that last one catalyse the nucleation of CNT crust covering the surface of AAO membranes.

Thus, in a nanotube wall formation the role of the localized (nickel) and injected catalyst, as well as the pore reconstructions in the formation of nanotubes inside AAO remain unclear. In order to shed some light on this phenomenon we conducted additional experiments. The results are presented for four types of samples (see Table 1 and Fig. 7).

DOI: 10.5963/AMSA0302001

TABLE 1 CONDITION OF EXPERIMENTS FOR THE ASSESSMENT OF INFLUENCE OF THE LOCALIZED CATALYST

Description of Sample	Conditions of Experiments	Type of Sample
Al_2O_3 membrane with or without Ni film	Annealing (820 ℃, 5 min, N_2 flow rate 100 cm^3/min)	A (no CNT)
Al_2O_3 membrane without Ni film	CVD in regime I after the AAO annealing in air (1000 ℃, 60 min)	B (no CNT)
Al_2O_3 membrane without Ni film	CVD in regime IV	C, D (CNT)
Al_2O_3 membrane with Ni film	CVD in regime IV	E, F (CNT)

From the presented data it is visible that neither the annealing process in inert atmosphere (i.e. reproducing of the synthesis conditions but without ferrocene/xylene supply) nor the CNT synthesis using the annealed in air AAO membranes gave rise to the nanotubes formation in the pores (Fig. 7(A, B)). On the other hand, carbon nanotubes were formed in the pores of pristine AAO no matter nickel did or did not deposit at the bottom of the pores (Fig. 7(C-F)). These results testify to the facts that 1) a localized catalyst (Ni) does not play any role in the formation on nanotubes in the AAO pores; 2) hydrocarbon from the gas phase penetrates into the AAO pores and is necessary for the nanotube formation; and 3) during the annealing in air some modifications of the pore structure/composition occur, which inhibit the nanotube growth in our synthesis conditions. It is possible that γ-Al_2O_3 transforms into α-Al_2O_3 (>950 ℃), which might be no longer favourable for the nanotube formation. The last assumption must be checked by conducting a more peculiar investigation. The role of Al_4C_3 and crystalline γ-Al_2O_3 in the formation of nanotubes also needs further study.

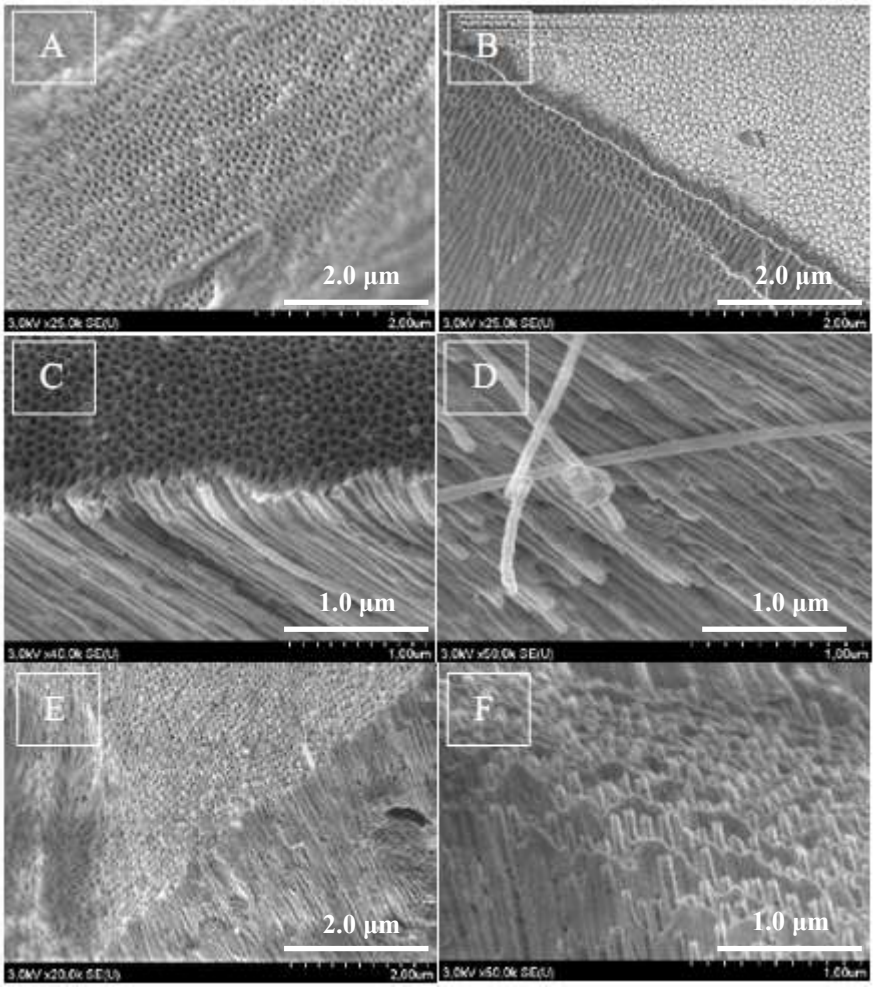

Fig. 7 Top and cross-sectional views of the samples: A – an AAO membrane annealed in N_2 atmosphere; B – an AAO membrane annealed in air followed by the CNT synthesis in regime I; C, D and E, F – CNT synthesis was carried out in regime I using AAO without and with Ni film, correspondingly. In all cases AAO was created by two-step anodizing and its thickness was about 40 µm

IV. CONCLUSIONS

In summary, the formation of carbon nanotubes in aluminium oxide membranes was investigated in various CVD conditions. It was found that relatively high catalyst concentrations inhibit the formation of nanotubes inside AAO, since a

DOI: 10.5963/AMSA0302001

thick CNT carpet is formed on the AAO membrane surface, which blocks the diffusion of reagents into the pores. Optimal conditions of CVD for the nanotube formation were found. It was established that neither deposited Ni nor iron from the ferrocene decomposition catalyses the formation of the nanotubes in AAO. Moreover, after the high-temperature annealing in air, AAO no longer supports the nanotubes formation in its pore by this method. We speculate that the formation of carbon nanotubes in the AAO pores is governed by the pore structure reconstruction (such as water desorption, phase transformation) during the high-temperature CVD process.

ACKNOWLEDGMENTS

The authors thank Prof. L.J. Balk and Dr. R. Heiderhoff (Bergische Universität Wuppertal) for the admission to the scanning electron microscope.

REFERENCES

[1] Tatsuya Iwasaki, Taiko Motoi, and Tohru Den, "Multiwalled carbon nanotubes growth in anodic alumina nanoholes," *Appl. Phys. Lett.*, vol. 75(14), pp. 2044-2047, Oct. 1999.

[2] W.I. Milne, K.B.K. Teo, G.A.J. Amaratunga, et al., "Carbon nanotubes as field emission sources," *Journal of Materials Chemistry*, vol. 14, pp. 933-938, 2004.

[3] A. Angelucci, A. Ciorba, L. Malferrari, F. Odorici, R. Rizzoli, M. Rossi, V. Sessa, M. Terranova, and G. Veronese, "Field emission properties of carbon nanotube arrays grown in porous anodic alumina," *Phys. Status Solidi (c)*, vol. 6, no. 10, pp. 2164-2169, 2009.

[4] D. Li, Y. Cheng, M. Cai, J. Yao, and P. Chang, "Uniform arrays of carbon nanotubes applied in the field emission devices," *Science China Physics, Mechanics and Astronomy*, vol. 56, pp. 2081-2088, 2013.

[5] R.J. Chen, S. Bangsaruntip, K.A. Drouvalakis et al. "Noncovalent functionalization of carbon nanotubes for highly specific electronic biosensors," *Proc. Nat. Acad. Sci. USA*, vol. 100, pp. 4984-4989, 2003.

[6] R. Mangu, S. Rajaputra, P. Clore, D. Qian, R. Andrews, and V.P. Singh, "Ammonia sensing properties of multiwalled carbon nanotubes embedded in porous alumina templates," *Materials Science and Engineering: B*, vol. 174, pp. 2-8, 2010.

[7] Z. Jin, F. Meng, J. Liu, M. Li, L. Kong, and J. Liu, "A novel porous anodic alumina based capacitive sensor towards trace detection of PCBs," *Sensors and Actuators B: Chemical*, vol. 157, pp. 641-645, 2011.

[8] H. Orikasa, N. Inokuma, S. Ittisanronnachai, X.H. Wang, O. Kitakami, and T. Kyotani, "Template synthesis of water-dispersible and magnetically responsive carbon nano test tubes," *Chem. Commun. (Cambridge)*, vol. 19, pp. 2215-2219, 2008.

[9] H. Gao, X. B. Wu, J. T. Li, G. T. Wu, J. Y. Lin, K. Wu, and D. S. Xu, "Hydrogen adsorption of open-tipped insufficiently graphitized multiwalled carbon nanotubes," *Appl. Phys. Lett*., vol. 83, pp. 3389-3394, 2003.

[10] S. H. Jeong and K. H. Lee, "Fabrication of the aligned and patterned carbon nanotube field emitters using the anodic aluminum oxide nano-template on a Si wafer," *Synth. Met*., vol. 139, pp. 385-390, 2003.

[11] W. K. Hu, L. M. Yuan, Z. Chen, D. Gong, and K. Saito, J., "Fabrication and characterization of vertically aligned carbon nanotubes on silicon substrates using porous alumina nanotemplates," *Nanosci. Nanotechnol*., vol. 2, pp. 203-207, 2002.

[12] H. Gao, C. Mu, F. Wang, D. Xu, K. Wu, Y. Xie, S. Liu, E. Wang, J. Xu, and D. Yu, "Field emission of large-area and graphitized carbon nanotube array on anodic aluminum oxide template," *J. Appl. Phys*., vol. 93, pp. 5602-5607, 2003.

[13] W. J. Yu, Y. S. Cho, G. S. Choi, and D. Kim, "Patterned carbon nanotube field emitter using the regular array of an anodic aluminium oxide template," *Nanotechnology*, vol. 16, pp. 291-295, 2005.

[14] H. Masuda, K. Fukuda, "Ordered metal nanohole arrays made by a two-step replication of honeycomb structures of anodic alumina," *Science*, vol. 268 (9), pp. 1466-1468, 1995.

[15] A. I. Vorobjova, B. G. Shulitskii, and E. L. Prudnikova, "Formation of template from anodic aluminum oxide to carbon nanotubes deposition," *Nano- Mikrosist. Tekh*., vol. 9, pp. 39-43, 2007.

[16] S. Esconjauregui, C. Whelan, and K. Maex, "The reasons why metals catalyze the nucleation and growth of carbon nanotubes and other carbon nanomorphologies," *Carbon*, vol. 47, pp. 659-669, 2009.

[17] S.-H. Jeong, H.-Y. Hwang, S.-K. Hwang, K.-H. Lee, "Carbon nanotubes based on anodic aluminum oxide nanotemplate," *Carbon*, vol. 42, pp. 2073-2080, 2004.

[18] X.T. Hoang, D.T. Nguyen, B.C. Dong, and H.N. Nguyen, "Advances in Natural Sciences," *Nanoscience and Nanotechnology*, vol. 4, p. 035013, 2013.

[19] A.S. Basaev, B.G. Shulitskii, A.I. Vorobjova, E.L. Prudnikova, V.A. Labunov, A.M. Mozalev, Yu.P. Shaman, V.N. Kukin, "Nanocomposite carbon material with ordered structure synthesized using anodic alumina oxide," *Nanotechnol. in Russia*, vol. 6(3-4), pp. 171-180, 2011.

[20] A.I. Vorobjova, B.G. Shulitskii, "Aligned carbon tubes synthesized using porous aluminum oxide," *Russian Microelectronics*, vol. 41(5), pp. 285-292, 2012.

DOI: 10.5963/AMSA0302001